Ionic Strength Dependent Binding Mode of 9-Aminoacridine to DNA

Hye-Kyung Kim, Tae-Sub Cho, and Seog K. Kim*

Department of Chemistry, College of Sciences, Yeungnam University, Kyoungsan, Kyoung-buk 712-749, Korea

Received December 18, 1995

The ionic strength dependent binding mode of 9-aminoacridine (9AA), a well-known DNA intercalator, to DNA is studied by flow linear dichroism, circular dichroism, fluorescence techniques and equilibrium dialysis. The DNA-bound 9AA exhibits spectral properties corresponding to the intercalative binding mode disregarding the salt concentrations; the angle between the long-axis transition moment of the 9AA molecule and DNA helix axis is calculated to be about 65°, indicating a significant deviation from the classical intercalation. At low salt concentrations, however, upwards bending curve in Stern-Volmer plot is observed (where 9AA is a fluorophore and DNA a quencher), indicating the coexistence of both static and dynamic quenching mechanisms or the existence of an additional binding site.

Introduction

DNA-intercalation of polycyclic aromatic compounds has been an interesting subject[1~3] due to their potentials as cytostatic reagents[4] and probes in molecular biology.[5] Binding to DNA by intercalation was originally explained by Lerman[6] as an intercalator is sandwiched between two adjacent base pairs. According to this model, the intercalator is coplanar with the base pairs and lengthens the helix by 3.4 Å corresponding to the van der Waals thickness of an aromatic intercalator, and simultaneously resulting in an unwinding of the DNA helix. The binding is in part due to disperse forces between the aromatic moieties of the bases and the intercalator. However, in most cases electrostatic interactions between the phosphates of the DNA backbone and cationic groups of the intercalator play a dominant role. The static interaction between DNA and several intercalators has been studied by X-ray diffraction using di- and oligonucleotide complexes[7,8] which confirmed the Lerman's model. Furthermore, the dynamic interactions between DNA and intercalators have been examined by various spectroscopic techniques, supporting the intercalation model.

9-Aminoacridine (9AA) is positively charged planar aromatic compound which make this molecule suitable DNA intercalator.[9~16] According to recent linear dichroism and electric orientation relaxation (EOR) study, however, the mode of intercalation of 9AA to DNA deviates from the classical intercalators in at least two aspects; elongation due to 9AA intercalation is 1.5 times compared to a classical intercalator ethidium and the long axis of the electric transition moment of 9AA tilts as much as 20° from the planes of DNA bases.[9,16] The possible reason for this deviation is either the intercalation mode itself that is different compared to a classical intercalator or binding heterogeneity in which the bound 9AA besides intercalated ones may contribute to the dichroism. In order to clarify this discrepancy, the ionic strength dependent spectroscopic properties, including linear dichroism (LD) and circular dichroism (CD), of the 9AA-DNA complex are investigated.

Materials and Methods

Materials. Highly polymerized calf thymus DNA, purchased from Pharmacia, was dissolved in 2 mM sodium phosphate buffer at pH 7.0 containing 20 mM NaCl and 1 mM EDTA followed by repeated dialysis against 2 mM sodium phosphate buffer at pH 7.0. This buffer was used throughout this work. 9AA was purchased from Sigma and used after recrystallization. The concentrations were determined using the molar absorptivities: $\varepsilon_{258nm}=6{,}700\ cm^{-1}\ M^{-1}$ and $\varepsilon_{400nm}=9{,}300\ cm^{-1}\ M^{-1}$, respectively for DNA and 9AA. Absorption spectra of the samples were recorded on a Cary 2300 spectrophotometer.

Circular dichroism (CD). CD is the differential absorption of circularly polarized light;

$$CD(\lambda)=A_l(\lambda)-A_r(\lambda) \tag{1}$$

where $A_l(\lambda)$ and $A_r(\lambda)$ are the absorbance measured with left and right circularly polarized light. CD of the ligand-DNA adduct systems provides information on two levels. Firstly, the conformation of DNA is represented through the CD of the intrinsic DNA absorption centered at 260 nm. Secondly, the environment of the bound ligand: although 9AA itself is achiral it acquires CD when bound to DNA.[9,17~21] The mechanism behind this induced CD is not clear but can be interpreted as the interaction between the non-degenerated transitions of 9AA and chirally arranged bases of the nucleic acid host and it is dependent upon the position and orientation of bound ligand with respect to the nucleo-bases of host DNA. All CD spectra were measured on a Jasco J-720 spectropolarimeter.

Linear dichroism (LD) and reduced linear dichroism (LD'). LD is defined as the differential absorption of the light polarized parallel ($A_\parallel$) and perpendicular ($A_\perp$) to some laboratory reference axis; in the case of flow LD, the parallel direction is the flow direction.[9] The LD data are evaluated as the *reduced linear dichroism*, LD', defined as:

$$LD'(\lambda)=\frac{LD(\lambda)}{A_{iso}(\lambda)} \tag{2}$$

where A_{iso} denotes the absorption spectrum for the isotropic sample. This dimensionless quantity is related to the orientation of the light absorbing transition moment as

$$LD'(\lambda)=S\times O=3S\frac{(<3\cos^2\alpha>-1)}{2} \tag{3}$$

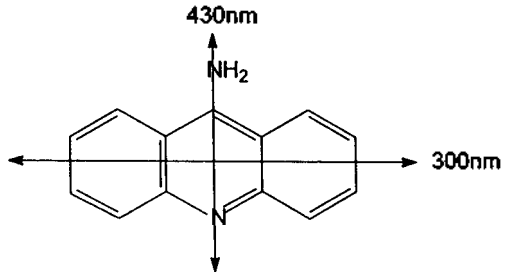

Figure 1. Molecular structure of 9AA.

where S is an orientation factor describing the degree of orientation of the DNA helix in the gradient shear. It depends on the contour length and flexibility of the DNA, flow rate, temperature, and viscosity of the medium.[9] The optical factor, O, reflects the angle α, between the transition moment of the bound ligand and the local DNA helix,[22,23] and the brackets denote an ensemble average over the angular distribution. The DNA bases have values close to 90°. Large values (80°-90°) for ligand are indicative of intercalation whereas values ranging from 40° to 50° are consistent with the transition lying along the minor groove. When several transitions are involved, the measurement of LD^r will be an average of the LD^r values of the individual transitions weighted with their respective absorbances. The $\pi\rightarrow\pi^*$ transitions of the DNA bases, that are responsible for the LD of the polynucleotide around 260 nm, are polarized in the plane of the bases with an effective angle $\alpha=86°$ between the plane of the bases and helix axis.[24,25] This angle is used to calculate the orientation factor, S, from the measured LD^r of the DNA bases. The LD spectra were recorded on a Jasco J-500A spectropolarimeter equipped with an Oxley prism to convert the circularly polarized light from the CD spectropolarimeter into linearly polarized light.[22]

Fluorescence quenching. Fluorescence quenching technique is utilized to study solvent accessibility to a fluorephore. A fluorescent probe that is protected from the solvent will not be quenched by the external quencher. This technique can also be used in order to probe the heterogeneity of the sample. In general the fluorescence quenching occurs through two mechanisms; diffusional and static quenching. Both can be described by the Stern-Volmer equation.[26]

$$\frac{F_o}{F}=1+K_{sv}[Q] \tag{4}$$

where F and F_o are the fluorescence intensities in the presence and absence of quencher, respectively, $[Q]$ denotes the quencher concentration and K_{sv} is the Stern-Volmer constant. K_{sv} is the product of the collisional rate constant and fluorescence lifetime of the quencher for diffusion controlled quenching process. For static processes in which the fluorophore loses its fluorescence by forming a non-fluorescent complex with quencher, K_{sv} denotes the equilibrium constant of the complex formation.

Upward bending curves in Stern-Volmer plot are often observed. These curves can generally be assigned to a two components system;[26]

$$\frac{F_o}{F}=(1+K_{sv1}[Q])(1+K_{sv2}[Q]) \tag{5}$$

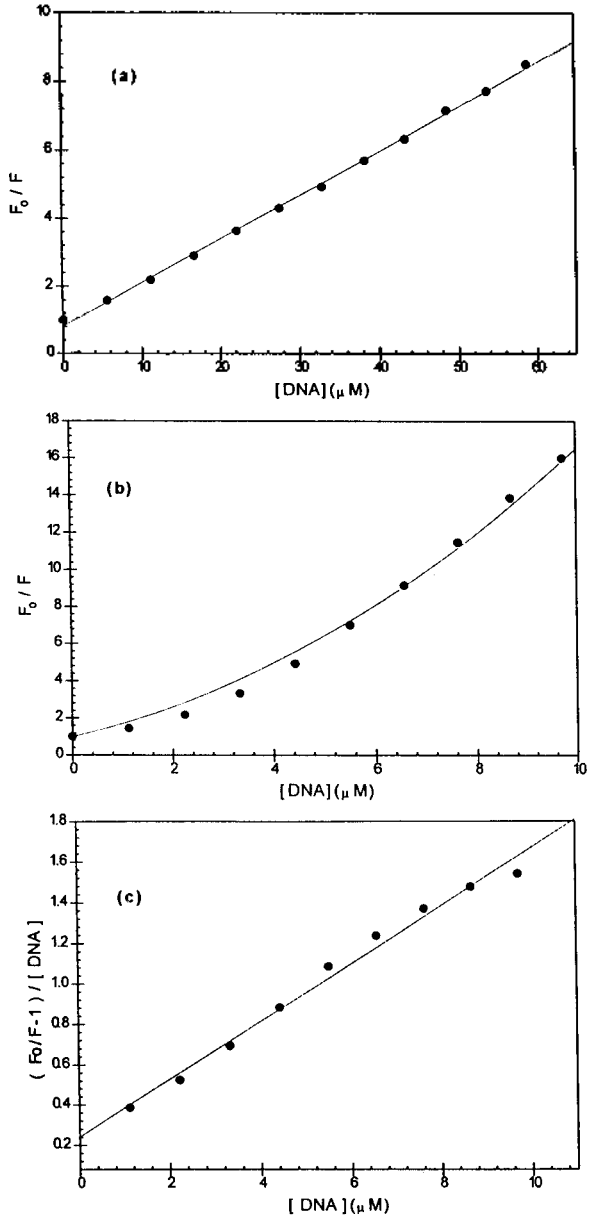

Figure 2. Stern-Volmer plot and modified Stern-Volmer plot. (a): Stern-Volmer plot of 9AA quenched by DNA in the high ionic strength. $[Na^+]=32$ mM. (b): Stern-Volmer plot of 9AA quenched by DNA in the low ionic strength. $[Na^+]=2$ mM. (c): modified Stern-Volmer plot of Figure 2(b).

where K_{sv1} and K_{sv2} denotes the equilibrium constants of independent binding site or static and dynamic quenching constant, respectively. Equation (6) can easily be deduced from equation (5) to give a straight line.

$$\frac{F_o/F-1}{[Q]}=K_{sv1}K_{sv2}[Q]-(K_{sv1}+K_{sv2}) \tag{6}$$

From the slope and intercept, K_{sv1} and K_{sv2} can be separated. Fluorescence spectra were measured on either an Aminco SPF-500 spectrofluorometer in the quantum corrected mode or a Perkin Elmer LS 50B spectrofluorometer. Absorbance of the samples for fluorescence measurements does not exceed than 0.1 to avoid inner filter effect.

Table 1. Binding constants of 9AA in the different sodium concentrations. ×: No second binding constant is detectable

[NaCl]	K_{SV_1}	K_{SV_2}
2 mM	2.82×10^5	3.34×10^6
4 mM	1.90×10^5	2.20×10^5
12 mM	0.72×10^5	1.33×10^5
32 mM	×	1.28×10^6
102 mM	×	0.32×10^5

Results and Discussion

Fluorescence Quenching

9AA is a highly fluorescent drug. When it is bound to DNA the fluorescence intensity decreases to a negligible magnitude, validating equations (5) and (6). Typical Stern-Volmer plot for the 9AA-DNA complex formation at representative high and low salt concentrations are depicted in Figure 2(a) and (b), respectively. The calculated values are also given in Table 1. A straight line in the Stern-Volmer plot is observed at high salt concentrations, strongly indicating the homogeneous binding of 9AA to DNA which is assigned to the intercalation (see below). The equilibrium constants are calculated to be 1.28×10^5 M^{-1} and 0.32×10^5 M^{-1} for the salt concentrations of 32 mM and 102 mM, respectively. These equilibrium constants are measured independently by equilibrium dialysis and are confirmed to be in the same range. On the other hand, at low salt concentrations, an upward bending curve is observed (Figure 2(b)), suggesting either binding heterogeneity of 9AA to DNA or two quenching mechanisms, namely dynamic and static mechanism is involved in the process. Two Stern-Volmer constants which can be seen the salt concentrations up to 12 mM are separated according to equation (6) (Figure 2(c) and Table 1). At the very low salt concentration (2 mM) the two constants are about the same: 2.82×10^5 M^{-1} and 3.34×10^5 M^{-1}. Three reasons can be conceivable for the Stern-Volmer constant which appears only at the low salt concentrations; (1) the spectroscopic properties of the bind 9AA at low salt concentration are so similar to those of the intercalated ones that optical spectroscopies can not distinguish. This possibility is highly unlikely because the fluorescence and CD are extremely sensitive to the environment of the DNA bound ligand, (2) 9AA binds to the surface of DNA resulting in the spectroscopic properties similar to the unbound ones, (3) the second binding we observe at low salt concentration is due to the dynamic mechanism in which 9AA and DNA does not form the complex resulting in no spectroscopic change. We do not have the solid evidence to distinguish between the second and third possibilities.

Spectroscopic Properties

Absorption. 9AA has two transition moments on the plane of the molecule which lie perpendicular to each other (Figure 1).[9,21] The short axis has a transition moment near 430 nm and long axis near 300 nm. When 9AA binds to DNA, the strong interaction between 9AA and DNA is recognized by hyphochromism (34%-43%) and red-shift (6 nm-7 nm) compared to the unbounded ones (Figure 3). An increase in salt concentration does not result in noticeable changes, indicating the interaction is not affected by salt concentration.

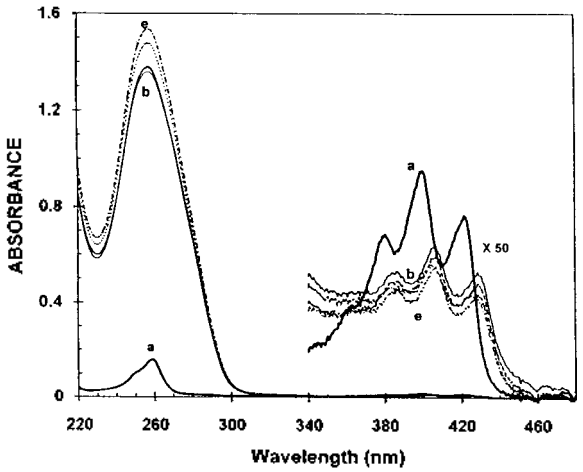

Figure 3. Absorption spectra of 9-AA complexed with double helical DNA in the different ionic concentrations. (a) free ligand spectrum of 9AA(2 μM) From (b) to (e): Complex of 9AA and DNA in the different sodium concentrations [9AA]=2 μM, [DNA]=200 μM and $[Na^+]$=2 mM, 7 mM, 20 mM, 102 mM.

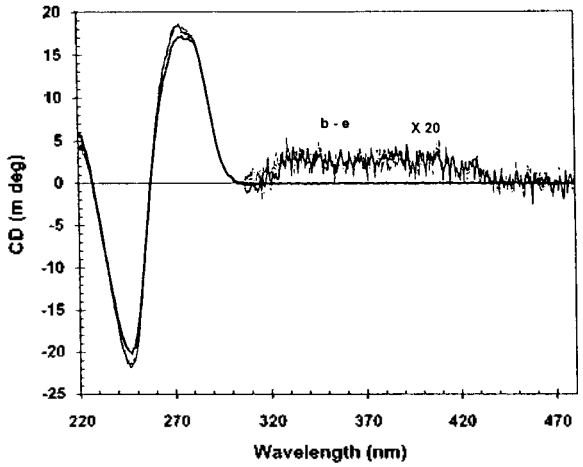

Figure 4. Induced CD spectra of 9AA complexed with double helical DNA. The concentrations are the same as in Figure 3.

CD. CD of the 9AA-DNA complex is depicted in Figure 4. Small changes in both DNA absorption region (220 nm-300 nm) and 9AA absorption region (300 nm-450 nm) can be seen. CD changes in DNA absorption region can be understood either due to the changes in the DNA conformation upon ligand binding or as an induced CD of bound 9AA. The origin of induced CD in this region cannot be fully explained at this point. CD in the long wavelength is that of the bound ligand. Although 9AA itself is achiral, interactions of the electric transition moments of 9AA with chirally arranged nuecleo-bases' transition moments acquire CD signal in ligand absorption region. In general, CD in ligand absorption region for the intercalator is weak and that of the minor groove binding ligand is strong (at least 10 times in magnitude) and positive.[19,20] The CD spectra in the long wavelength

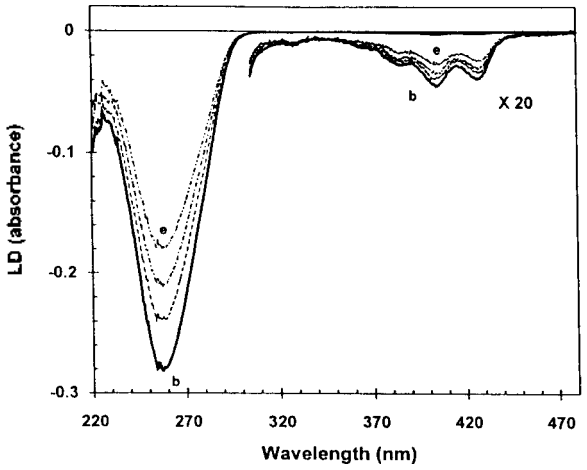

Figure 5. LD spectra of 9AA complexed with DNA. The concentrations are the same as in Figure 3.

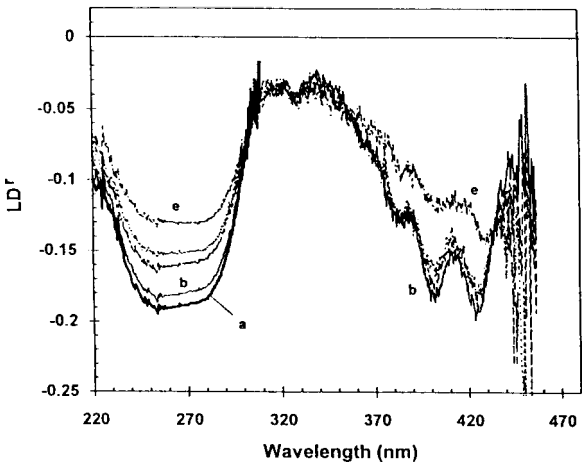

Figure 6. LD' spectra of 9AA complexed with DNA. free DNA is shown as thick solid curve. The concentrations are the same as in Figure 3.

recorded for the 9AA-DNA complexes at low and high salt concentrations are coincidentally the same, indicating the binding mode is independent of salt concentration (Figure 4). The magnitude in this region is small, suggesting 9AA is intercalated between the DNA bases.

LD and LD'. Figure 5 shows LD spectra of the 9 AA-DNA complexes at various salt concentrations. Negative LD signal in the ligand absorption region indicates the angle between transition moments of bound 9AA and the DNA helix axis is larger than 54.7° which immediately removes the possibility of the groove binding. The magnitude of LD in the DNA absorption region decreases with increasing salt concentration. The salt ions bind to phosphate and decrease the electrostatic repulsion between the phosphate groups thereby increase the flexibility of DNA which make hard for DNA to be aligned in the shear gradient.

LD' signals of the 9AA-DNA complexes show that both DNA and ligand absorption regions are negative (Figure 6). Moreover, the magnitude in the 260 nm region and 370 nm-420 nm is the same, indicating the short axis transition moment of 9AA and the DNA helix axis is almost perpendicular. On the other hand, the angle between the long axis of the 9AA molecule and DNA helix axis is calculated to be about 65°, assuming the average angle of the DNA bases with respect to DNA helix axis is 86°. The magnitude of LD' in the absorption region of both long and short axis remains to be constant, indicating the binding geometry of 9AA when complexed with DNA is not affected by the ionic strength. The tilt angle of about 65° of the long axis electric transition moment of 9AA coincides with the base tilt angle, therefore, one may suggest that the 9AA molecule inserts itself between the DNA base pairs in the manner that short axis is perpendicular and long axis tilt about 20° relative to the planes of DNA bases.

It is noteworthy that when a classical intercalator such as ethidium bromide is intercalated between DNA base pairs, the magnitude of LD and LD' increases due to lengthening and stiffening of DNA itself (see equations (2) and (3)). What we observed here is that the magnitude of LD' of the 9AA-DNA complex remains the same at the same ionic strength (data not shown). Hence, upon 9AA binding to DNA, the unwinding and stiffness of DNA does not contribute to the LD signal, which differs from the EOR results,[14,16] in which 1.5 times base thickness elongation per 9AA intercalation has been reported.

Conclusion

At low salt concentration, the binding of 9AA to DNA is heterogeneous. In addition to the reported intercalation mode, fluorescence quenching technique suggests the possibility of the outside binding in which positively charged 9AA is associated randomly with the negatively charged DNA phosphate group or the fluorescence of 9AA is simply quenched by dynamic processes. Intercalative binding geometry of 9AA to DNA which is found to be independent of ionic strength is confirmed to be different compared to that of classical intercalation mode.

Acknowledgment. This work is supported by the Korea Science and Engineering Foundation (Grant No. 941-0330-020-2).

References

1. Capelle, N.; Barbet, J.; Dessen, P.; Blanguet, S.; Roques, B. P.; Le Pecq, J. B. *Biochemistry* **1979**, *15*, 3354.
2. Shafer, R. H.; Waring, M. J. *Biopolymer* **1980**, *19*, 431.
3. Waring, M. J. *Ann. Rev. Biochem.* **1981**, *50*, 159.
4. Topal, M. D. *Biochemistry* **1981**, *23*, 2367.
5. Wirth, M.; Ygge, B.; Buchardt, O.; Nielsen, P. E.; Nordén, B. *Photochem. Photobiol.* **1986**, *44*, 587.
6. Lerman, L. S. *J. Mol. Biol.* **1961**, *3*, 18.
7. Wang, A. H. J.; Ughetto, G.; Quigley, G. J.; van der Marel, G. A.; van Boom, J. H.; Rich, A. *Science* **1984**, *225*, 1115.
8. Ughetto, G.; Wang, A. H. J.; Quigley, G. J.; van der Marel, G. A.; van Boom, J. H.; Rich, A. *Nucl. Acids Res.* **1985**, *13*, 2305.
9. Nordén, B.; Kubista, M.; Kurucsev, T. *Quart. Rev. Biophys.* **1992**, *25*, 51.
10. Flock, S.; Bailly, F.; Bailly, C.; Waring, M. J.; Hénichart, J-P.; Coloson, P.; Houssier, C. *J. Biomol. Str. Dyn.* **1994**,

11, 881.
11. Assa-Munt, N.; Denny, W. A.; Leupin, W.; Kearns, D. R. *Biochemistry* **1985**, *24*, 1441.
12. Assa-Munt, N.; Denny, W. A.; Leupin, W.; Kearns, D. R. *Biochemistry* **1985**, *24*, 1449.
13. Le Pecq, J-B.; Le Bret, M.; Barbet, J.; Roques, B. *Proc. Natl. Acad. Sci. U.S.A.*, **1975**, *72*, 2915.
14. Wirth, M.; Buchard, O.; Koch, T.; Nielsen, P. E.; Nordén, B. *J. Am. Chem. Soc.* **1988**, *110*, 932.
15. Atwell, G. J.; Leupin, W.; Twigden, S. J.; Denny, W. A. *J. Am. Chem. Soc.* **1983**, *105*, 2913.
16. Hansen, J. B.; Koch, T.; Buchardt, O.; Nielsen, P. E.; Wirth, M.; Nordén, B. *Biochemistry* **1983**, *22*, 4878.
17. Nordén, B.; Tjerneld, F. *Biochemistry* **1982**, *21*, 1713.
18. Kubista, M.; Åkerman, B.; Albinsson, B. *J. Am. Chem. Soc.* **1989**, *111*, 7031.
19. Lyng, R.; Rodger, A.; Nordén, B. *Biopolymers* **1991**, *31*, 1709.
20. Lyng, R.; Rodger, A.; Nordén, B. *Biopolymers* **1992**, *32*, 1201.
21. Schipper, P. E.; Nordén, B. *Chem. Phys. Letters* **1979**, *67*, 99.
22. Nordén, B.; Seth, S. *Appl. Spectrosc.* **1985**, *39*, 647.
23. Nordén, B.; Kurucsev, T. *J. Mol. Recog.* **1994**, *7*, 141.
24. Matsuoka, Y.; Nordén, B. *Biopolymers* **1982**, *21*, 2433.
25. Matsuoka, Y.; Nordén, B. *Biopolymers* **1983**, *22*, 1731.
26. Lakowicz, J. R. *Principles of Fluorescence Spectroscopy*; Plenum Press: New York, U.S.A., 1983; p 257.

1-(*p*-Substituted)benzyl-1,1-dimethyl-2-(*p*-substituted)benzoyl Hydrazinium Hexafluoroantimonates as Useful Catalysts for the Acetalization of Carbonyl Compounds with Diols

Sang-Bong Lee*, Hyein Jung, and Kyu Wan Lee

Catalysis Research Division, Korea Research Institute of Chemical Technology, P.O. Box 107, Yusong, Taejon 305-600, Korea

Received December 28, 1995

Carbonyl compounds **1**, alkyl- and arylaldehydes and alkyl, aryl, benzylic, and cyclic ketones were converted to the corresponding 1,3-dioxolanes **2** and 1,3-dioxanes **4** with ethylene glycol and 2,2-dimethyl-1,3-propanediol in the presence of 1-3 mol% of 1-(*p*-substituted)benzyl-1,1-dimethyl-2-(*p*-substituted)-benzoyl hydrazinium hexafluoroantimonates **3** in high yields.

Introduction

The carbonyl function, as present in aldehydes and ketones, is probably one of the most versatile functional groups in organic chemistry; and not surprisingly a great deal of work has been done on the protection and masking of the carbonyl compounds. The formed acetal derivatives are important intermediates or end product in synthetic organic chemistry. One of the most convenient and practical methods for the syntheses of acetals from aldehydes and ketones is to react carbonyl compounds with diols such as ethylene glycol in the presence of an appropriate acidic catalyst with azeotropic removal of water formed by reflux solvent immisible with water.[1]

p-Toluenesulfonic acid (TsOH) is usually used as an acid catalyst,[2,3] while pyridinium *p*-toluenesulfonate is one of the mild catalysts[4] for acid sensitive carbonyl compounds. Generally, the catalysts used for acetalization are not easy to handle due to their hygroscopicity.

We have developed a new class of Lewis acid catalysts, *N*-benzyl group containing pyridinium salts that are characterized by their ease of synthesis and handling due to their reduced hygroscopicity and their chemical stability toward air, water, and organic solvents (e.g., they can be recrystallized from methanol). These salts are conceived to induce benzyl cations by heating to initiate the polymerizations of cyclic ethers[5,6] and a vinyl monomer[7] and to catalyze organic reactions, acetalizations of carbonyl compounds with epoxides[8] or diols.[9]

Recently, we reported a new class of Brønsted acid-inducing catalyst, 1-(*p*-substituted)benzyl-1,1-dimethyl-2-(*p*-substituted)benzoylhydrazinium hexafluoroantimonates **3** of which significances are evaluated as the same as that of *N*-benzyl group containing pyridinium salts in addition to their thermal latency.[10]

In this article, synthesis and the use of **3** as catalysts for the acetalization of carbonyl compounds with ethylene glycol and 2,2-dimethyl-1,3-propandiol are described.

Experimentals

Materials. Commercially available extra pure grade 1,1-dimethylhydrazine, benzoyl chloride, *p*-nitrobenzoyl chloride, benzyl bromide, *p*-methoxybenzyl alcohol, 47% of hydrogen bromide, 98% sulfuric acid, sodium hexafluoroantimonate, benzaldehyde, cyclohexanone, acetophenone, benzophenone,